SYNTHESIS, BIOLOGICAL EVALUATION AND LIGAND BASED PHARMACOPHORE MODELING OF NEW AROMATIC THIOSEMICARBAZONES AS POTENTIAL ANTICANCER AGENTS

**A. Karaküçük-İyidoğan,[1,*] B. Aydınöz,[1] T. Taşkın-Tok,[1]
E. E. Oruç-Emre,[1] and J. Balzarini[2]**

Two series of new aromatic thiosemicarbazone derivatives were synthesized by condensation of *N*-(4-cyanophenyl)hydrazine carbothioamide (**I**) and *N*-(4-methylsulfanylphenyl)hydrazine carbothioamide (**II**) with appropriate aromatic aldehydes in order to investigate their antiviral and cytostatic potency. The chemical structures of all compounds were fully characterized by elemental analysis and spectroscopic techniques. The results of the bioassays indicated that compounds **Id**, **Ie**, **If** and **IIf** proved inhibitory against influenza virus A (EC_{50} = 13 – 27 μg/mL for strain H1N1 and 9.3 – 18 μg/mL for strain H3N2). Compounds **Ig** and **IIg** were the most cytostatic compounds with inhibition of HeLa cell proliferation at an IC_{50} = 0.3 μg/mL for **Ig** and 1.9 μg/mL for **IIg**. Especially, compound **Ig** showed the highest cytostatic activity with IC_{50} of 0.30, 0.70 and 2.50 μg/mL against HeLa, CEM and L1210 cell lines, respectively. This inhibition range was within the same order of magnitude as that for cisplatin. Furthermore, molecular modeling was carried out to examine the cytostatic activity and determine the best pharmacophore model as a guide for the design and development of potential prodrugs in future studies.

Keywords: aromatic thiosemicarbazone; antiviral activity; cytostatic activity; anti-influenza activity; pharmacophore modeling.

1. INTRODUCTION

Thiosemicarbazones are important class of synthetic products and potential biologically active compounds. Domagk, et al. [1] first reported that thiosemicarbazone pharmacophore had antituberculosis activity. Then, antiviral activity of benzaldehyde thiosemicarbazone derivatives against vaccina virus in mice was found by Hamre, et al. [2]. The antiviral activity of isatin-β-thiosemicarbazone (IBT) and *N*-methyl-isatin-β-thiosemicarbazone (commercially known as Methisazone or Marboran) was widely investigated against orthopoxviruses in the 1960s [3]. After these discoveries, thiosemicarbazones draw considerable interest due to their application in the pharmaceutical chemistry and proved to be chemotherapeutic agents potentially useful for inhibiting cancer cells [4]. For example, 3-aminopyridine-2-carboxaldehyde thiosemicarbazone (commercially known as

Triapine) inhibited the biosynthesis of DNA in murine leukemia L1210 cells by blocking the activity of ribonucleotide reductase [5].

In recent years, it has been commonly accepted that agents containing more than one pharmacophore can have superior efficacy as compared to single-pharmacophore drugs [6]. Pharmacophore hybridization is a method of rational drug design, and a single molecule containing different modes of action can be beneficial for the treatment of diseases. As an important pharmacophore, bis-alkylating nitrogen mustard such as chlormethine, melphalan, chlorambucil and many more have anticancer activities against hematologic tumors, myeloma, ovarian cancer and solid tumors [7]. Alkylating agents are electrophilic entities that interact with nucleophilic moieties of DNA resulting in the covalent transfer of an alkyl group. Another pharmacophore *para*-substituted aryl nitrile, which is bioisostere of a ketone group, has a variety of anticancer activities, e.g., against hormonally-responsive breast cancer (letrozole), breast cancer (neratinib), prostate cancer (bicalutamide), pancreatic cancer, non-small cell lung cancer, head and neck cancer (L-778,123, phase I),

[1] Department of Chemistry, Gaziantep University, 27310 Gaziantep, Turkey.
[2] Laboratory of Virology and Chemotherapy, Rega Institute for Medical Research, KU Leuven, 3000 Leuven, Belgium.
[*] e-mail: iyidogan@gantep.edu.tr
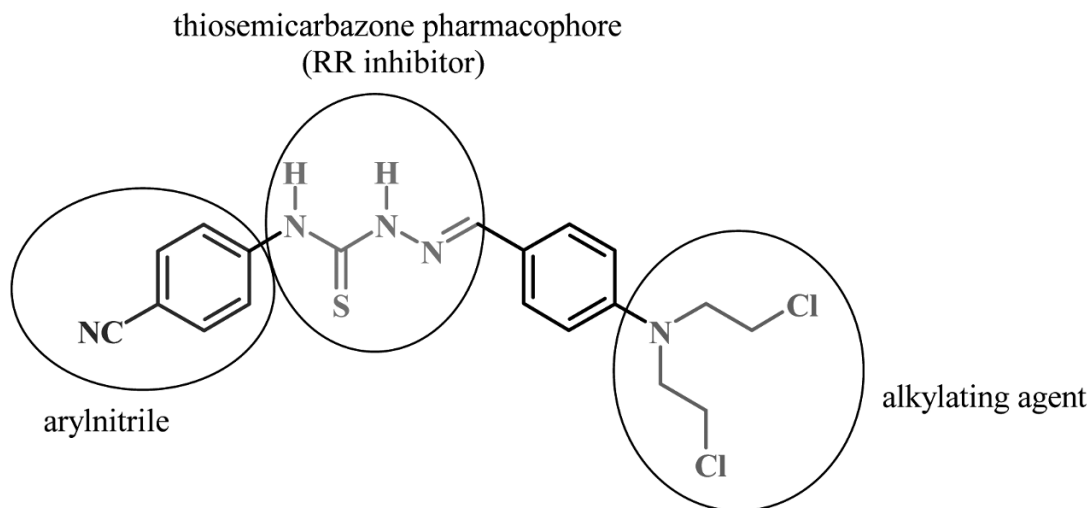
Fig. 1. Design of compound **Ig**.

and chronic myelogenous leukemia (bosutinib, SKI-606, phase III) [8].

Previously, we reported *in vitro* cytostatic and broad-spectrum antiviral activity of the thiosemicarbazones derived from 5-substitutedthiophene-2-carboxaldehydes and their platinum(II) and palladium(II) complexes [9]. Encouraged by these results and aimed at developing effective anticancer agents, we designed two series of thiosemicarbazones by the pharmacophore hybridization method using two or more different pharmacophores in view of prospecting their cytostatic and antiviral activity (Fig. 1). In order to gain detailed information about this issue and to develop effective anticancer agents for future studies, we have performed virtual screening of the aforementioned compounds by using Gaussian09 and Discovery Studio 3.5 software [10, 11].

The intermediates *N*-(4-cyanophenyl)hydrazinecarbothioamide (**I**) and *N*-(4-methylthiophenyl)hydrazinecarbothioamide (**II**) were prepared from 4-cyanophenyl isothiocyanate and 4-methylthiophenyl isothiocyanate by reaction with hydrazine monohydrate, respectively [12]. *N*-(4-cyanophenyl)hydrazinecarbothioamide (**I**) was reported previously [13] and *N*-(4-methylthiophenyl)hydrazinecarbothioamide (**II**) was commercially available. The novel thiosemicarbazones (**Ia – Ig** and **IIa – IIg**) as well as the known analog of **Ib** [14] were synthesized in high yield (71 – 92%) from the corresponding 4-substitutedbenzaldehydes by treatment with thiosemicarbazides in methanol, according to the general procedure of a previously described method [15]. The synthetic route of target compounds **Ia – Ig** and **IIa – IIg** is shown in Scheme 1.

The chemical structures of new compounds were throughly eludicated by elemental analysis and spectral data (UV-Vis, IR, ¹H NMR, ¹³C NMR, and ESI-MS). Assignments of selected diagnostic IR bands provided significant indication for the formation of the thiosemicarbazone deriva-

tives. All thiosemicarbazone derivatives (**Ia-g** and **IIa-g**) exhibited two intense bands in the region of 3396 – 3266 cm⁻¹ and 3162 – 3120 cm⁻¹ due to ν(N-H) stretching. The strong band at 839 – 818 cm⁻¹ was present due to ν(C=S) stretching. It was suggested that thiosemicarbazones in the solid phase remain in the thione form. In addition, the characteristic azomethine stretching vibrations ν(C=N) at 1587 – 1543 cm⁻¹ were observed, which also confirmed the formation of thiosemicarbazones [16]. Results of the ¹H NMR integrations and signal multiplicities were in line with the proposed structures and other spectral data. The ¹H NMR spectra of **Ia – Ig** and **IIa – IIg** showed a singlet peak attributable to the =N-NH proton in arange of δ = 12.60 – 11.62 ppm as well as a singlet peak attributable to the PhNH proton in the range δ = 10.80 – 9.92 ppm. The signal of the azomethine proton (HC=N) appeared as a singlet at δ = 8.63 – 8.04 ppm [16]. All aromatic protons were observed with the expected chemical shift (δ = 8.48 – 6.80 ppm) and coupling constant in the NMR spectra of all thiosemicarbazone derivatives. The ¹³C NMR spectra of the thiosemicarbazones exhibited two important signals at δ = 176.92 – 174.23 and at δ = 143.89 – 142.57 ppm assigned to thioamide (C=S) and imine (C=N) carbon atoms, respectively. The signals at δ = 164.01 – 112.06 ppm in the spectra were assumed to be due to the aromatic carbons. The MS spectra of all thiosemicarbazones were in line with the proposed structures.

2. EXPERIMENTAL CHEMICAL PART

The progress of all reactions were monitored by thin layer chromatography (TLC). TLC was performed on silica gel plates (Merck Silica Gel 60, F₂₅₄, 0.2 mm) with visualization by exposure to iodine vapor and UV light using
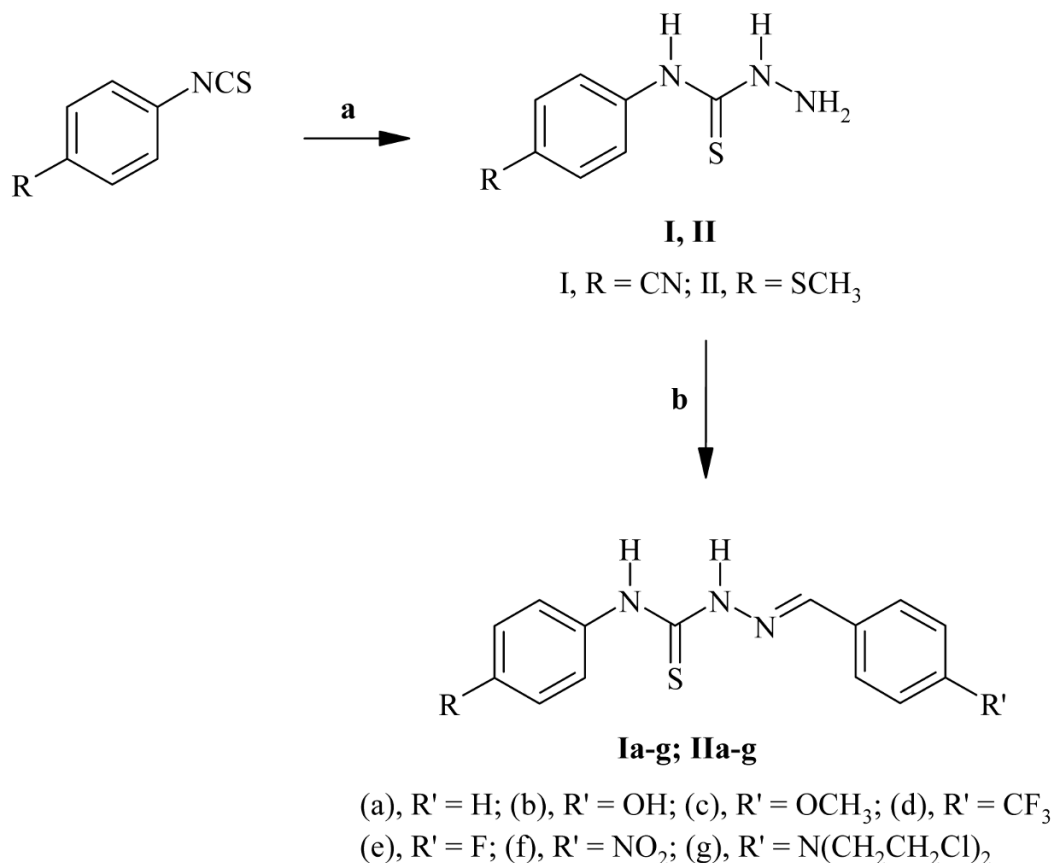
Scheme 1. Synthetic pathway of thiosemicarbazones **Ia – Ig** and **IIa – IIg.** Reagents and conditions: (a) NH$_2$NH$_2$.H$_2$O (98%), Et$_2$O, rt, 24 h; (b) appropriate aldeyhde in MeOH, reflux.

EtOAc/hexane (v/v 1:1 and 1:3) as solvent system. Melting points were determined on a EZ-Melt MPA120 Automated Melting Point apparatus and were uncorrected. The IR spectra were recorded on a Perkin Elmer 100 FT-IR spectrometer with universal ATR sampling accessory. The ^{1}H NMR and ^{13}C NMR spectra were obtained at room temperature with a Bruker Avance-DPX-400 NMR spectrometer in DMSO-d_6 using TMS as the internal standard. The mass spectra were obtained using an LC/MS Agilent 1100 MSD series spectrometer in the electrospray mode. Elemental (CHNS) analyses were performed using a VarioMICRO elemental analyzer.

2.1. Synthesis of Thiosemicarbazides I and II

General procedure. A solution of hydrazine monohydrate (7.50 mmol) in diethylether (20 mL) was added dropwise to a solution of 4-substitutedphenyl isothiocyanate (6.25 mmol) in diethyl ether (20 mL) at room temperature with vigorous stirring. The mixture was allowed to stand overnight. The precipitated solid was filtered and washed two times with water. The crude product was recrystallized from methanol.

N-(4-cyanophenyl)hydrazinecarbothioamide (I). Light yellow solid (methanol). Yield: 1.14 g (95%); m.p.: 185 – 186°C. Anal. calc. for C$_8$H$_8$N$_4$S: C, 49.98; H, 4.19; N, 29.14; S, 16.68%. Found: C, 49.86; H, 4.29; N, 29.16; S, 16.84%. UV (DMSO, λ$_{max}$, nm): 325; 293; 236. IR (ν$_{max}$, cm^{-1}): 3338, 3196 (N-H); 2229 (C≡N); 1208 (C-N); 1083 (N-N); 831 (C=S). ^{1}H NMR (DMSO-d_6; δ, ppm): 9.53 (s, 1H, N*H*NH$_2$); 9.40 (s, 1H, PhN*H*); 8.10 (d, 2H, Ar*H*, J = 8.23 Hz, *orto* protons to -CN group); 7.76 (d, 2H, Ar*H*, J = 8.26 Hz, *meta* protons to -CN group); 4.99 (brs, 2H, N*H$_2$*).

N-(4-methylsulfanylphenyl)hydrazinecarbothioamide (II). White solid (methanol). Yield: 1.17 g (88%); m.p.: 181 – 182°C. Anal. calc. for C$_8$H$_{11}$N$_3$S$_2$: C, 45.04; H, 5.20; N, 19.70; S, 30.06%. Found: C, 45.24; H, 5.43; N, 19.63; S, 30.07%. UV (DMSO, λ$_{max}$, nm): 330; 293; 237. IR (ν$_{max}$, cm^{-1}): 3346, 3274, 3175 (N-H); 1203 (C-N); 1064 (N-N); 828 (C=S). ^{1}H NMR (DMSO-d_6; δ, ppm): 9.60 (s, 1H, N*H*NH$_2$); 9.12 (s, 1H, PhN*H*); 7.59 (d, 2H, Ar*H*, J = 8.57 Hz, *meta* protons to -SCH$_3$ group); 7.21 (d, 2H, Ar*H*, J = 8.61 Hz, *orto* protons to -SCH$_3$ group); 4.80 (brs, 2H, N*H$_2$*); 2.46 (s, 3H, SC*H$_3$*).

2.2. Synthesis of Thiosemicarbazones Ia – Ig and IIa – IIg

General procedure: To a hot solution of thiosemicarbazide (1.04 mmol) in methanol (25 mL) was added dropwise a solution of the appropriate aldehyde (1.04 mmol) in methanol (10 mL) with continuous stirring. After the addition of a catalytic amount of glacial acetic acid, the reaction mixture was refluxed for 6 – 24 h. The progress of the reaction was monitored by TLC. The reaction mixture was cooled and the precipitate was filtered. The crude product was washed with cold diethylether or ethanol and recrystallized from appropriate solvent. Table 1 presents data of mass spectroscopy and elemental analysis for aromatic thiosemicarbazones **Ia – Ig** and **IIa – IIg**.

2-Benzylidene-*N*-(4-cyanophenyl)hydrazinecarbothioamide (Ia). Yellow solid (acetone). Yield: 0.26 g (90%); m.p.: 193 – 194°C. IR (ν_{max}, cm^{-1}): 3275, 3140 (N-H); 2220 (C≡N); 1580 (C=N); 1200 (C-N); 1063 (N-N); 834 (C=S). ^{1}H NMR (DMSO-d_6; δ, ppm): 12.10 (s, 1H, CSN*H*); 10.33 (s, 1H, PhN*H*); 8.22 (s, 1H, *H*C=N); 7.97 (d, 2H, Ar*H*,

$J = 8.62$ Hz, *orto* protons to -CN group); 7.91 (dd, 2H, Ar*H*, $J_1 = 3.58$ Hz, $J_2 = 2.40$ Hz, orto protons at phenyl ring); 7.83 (d, 2H, Ar*H*, $J = 8.62$ Hz, *meta* protons to -CN group); 7.46 (t, 3H, Ar*H*, $J_1 = 3.42$ Hz, $J_2 = 2.93$ Hz, *para* and *meta* protons at phenyl ring). ^{13}C NMR (DMSO-d_6; δ, ppm): 176.49 (*C*=S), 143.78 (*C*=N), 141.99, 133.83, 132.34, 131.75, 130.16, 129.13, 128.55, 118.67 (Ar*C*), 108.62 (C≡N).

2-(4-Hydroxybenzylidene)-*N*-(4-cyanophenyl)hydrazinecarbothioamide (Ib). Yellow solid (acetone). Yield: 0.22 g (71%); m.p.: 224 – 225°C. IR (ν_{max}, cm^{-1}): 3396, 3153 (O-H and N-H); 2229 (C≡N); 1579 (C=N); 1207 (C-N); 1060 (N-N); 833 (C=S). ^{1}H NMR (DMSO-d_6; δ, ppm): 11.93 (s, 1H, CSN*H*); 10.20 (s, 1H, PhN*H*); 9.98 (s, 1H, O*H*); 8.10 (s, 1H, *H*C=N); 7.98 (d, 2H, Ar*H*, $J = 8.69$ Hz, *orto* protons to -CN group); 7.82 (d, 2H, Ar*H*, $J = 8.67$ Hz, *meta* protons to -CN group); 7.74 (d, 2H, ArH, $J = 8.64$ Hz, *meta* protons to -OH group); 6.82 (d, 2H, Ar*H*, $J = 8.64$ Hz *orto* protons to -OH group). ^{13}C NMR (DMSO-d_6; δ, ppm): 175.56 (*C*=S), 154.42 (Ar*C, ipso* car-

TABLE 1. Molecular Formulas, Mass Spectroscopy Data and Elemental Analysis of Aromatic Thiosemicarbazones **Ia-Ig** and **IIa-IIg**

Compd	R	R′	Molecular formula	MS (*m/z*)	% Elemental analysis of C, H, N, S: Found (Calcd.)			
					C	H	N	S
Ia	-CN	-H	$C_{15}H_{12}N_4S$	279.1 [M-H]$^-$	64.47 (64.26)	4.48 (4.31)	19.76 (19.98)	11.39 (11.44)
Ib	-CN	-OH	$C_{15}H_{12}N_4OS$	295.1 [M-H]$^-$	60.45 (60.79)	4.18 (4.08)	18.65 (18.91)	10.41 (10.52)
Ic	-CN	-OCH$_3$	$C_{16}H_{14}N_4OS$	309.1 [M-H]$^-$	61.99 (61.92)	4.98 (4.75)	18.35 (18.05)	10.14 (10.33)
Id	-CN	-OCF$_3$	$C_{16}H_{11}F_3N_4OS$	363.1 [M-H]$^-$	52.68 (52.74)	3.04 (3.21)	15.78 (15.58)	8.95 (8.80)
Ie	-CN	-F	$C_{15}H_{11}FN_4S$	298.1 [M]$^+$	60.04 (60.29)	3.42 (3.52)	18.53 (18.78)	10.92 (10.75)
If	-CN	-NO$_2$	$C_{15}H_{11}N_5O_2S$	324.1 [M-H]$^-$	55.23 (55.38)	3.92 (3.81)	21.85 (21.63)	9.97 (9.86)
Ig	-CN	-N(CH$_2$CH$_2$Cl)$_2$	$C_{19}H_{19}Cl_2N_5S$	419.0 [M-H]$^-$	54.24 (54.29)	4.36 (4.56)	16.82 (16.66)	7.34 (7.63)
IIa	-SCH$_3$	-H	$C_{15}H_{15}N_3S_2$	300.1 [M-H]$^-$	59.65 (59.77)	5.27 (5.02)	13.73 (13.84)	21.23 (21.28)
IIb	-SCH$_3$	-OH	$C_{15}H_{15}N_3OS_2$	316.0 [M-H]$^-$	56.90 (56.76)	4.98 (4.76)	13.52 (13.34)	20.44 (20.20)
IIc	-SCH$_3$	-OCH$_3$	$C_{16}H_{17}N_3OS_2$	330.1 [M-H]$^-$	57.62 (57.78)	5.34 (5.27)	12.80 (12.68)	19.26 (19.35)
IId	-SCH$_3$	-OCF$_3$	$C_{16}H_{14}F_3N_3OS_2$	384.0 [M-H]$^-$	49.68 (49.86)	3.87 (3.66)	10.84 (10.90)	16.64 (16.64)
IIe	-SCH$_3$	-F	$C_{15}H_{14}FN_3S_2$	319.1 [M]$^+$	56.12 (56.30)	4.71 (4.62)	13.58 (13.28)	20.37 (20.08)
IIf	-SCH$_3$	-NO$_2$	$C_{15}H_{14}N_4O_2S_2$	345.0 [M-H]$^-$	52.68 (52.41)	4.49 (4.27)	16.72 (16.47)	18.93 (18.72)
IIg	-SCH$_3$	-N(CH$_2$CH$_2$Cl)$_2$	$C_{19}H_{22}Cl_2N_4S_2$	440.1 [M-H]$^-$	51.69 (51.70)	5.28 (5.02)	12.39 (12.49)	14.47 (14.53)

bon to -OH group), 143.48 ($\underline{C}$=N), 141.98, 132.64, 131.73, 130.21, 127.47, 119.44, 116.72 (Ar$\underline{C}$), 107.52 (C≡N).

2-(4-Methoxybenzylidene)-*N*-(4-cyanophenyl)hydrazinecarbothioamide (Ic). Beige solid (ethanol). Yield: 0.29 g (92%); m.p.: 217 – 218°C. IR (ν_{max}, cm^{-1}): 3273, 3158 (N-H); 2227 (C≡N); 1543 (C=N); 1201 (C-N); 1022 (N-N); 835 (C=S). ^{1}H NMR (DMSO-d_6; δ, ppm): 12.03 (s, 1H, CSN$\underline{H}$); 10.25 (s, 1H, PhN$\underline{H}$); 8.15 (s, 1H, $\underline{H}$C=N); 7.97 (d, 2H, Ar$\underline{H}$, J = 8.73 Hz, *orto* protons to -CN group); 7.85 (d, 2H, Ar$\underline{H}$, J = 8.83 Hz, *meta* protons to -OCH$_3$ group); 7.82 (d, 2H, Ar$\underline{H}$, J = 8.70 Hz, *meta* protons to -CN group); 7.01 (d, 2H, Ar$\underline{H}$, J = 8.81 Hz, *orto* protons to -OCH$_3$ group); 3.81 (s, 3H, OC$\underline{H}_3$). ^{13}C NMR (DMSO-d_6; δ, ppm): 176.38 ($\underline{C}$=S), 158.32 (Ar$\underline{C}$, *ipso* carbon to -OCH$_3$ group), 143.76 ($\underline{C}$=N), 142.58, 140.35, 133.09, 129.17, 126.76, 124.86, 119.49 (Ar$\underline{C}$), 106.98 (C≡N), 56.12 (O$\underline{C}$H$_3$).

2-[(4-Trifluoromethoxy)benzylidene]-*N*-(4-cyanophenyl)hydrazinecarbothioamide (Id). White solid (acetone). Yield: 0.28 g (72%); m.p.: 219 – 220°C. IR (ν_{max}, cm^{-1}): 3291, 3149 (N-H); 2223 (C≡N); 1549 (C=N); 1201 (C-N); 1079 (N-N); 839 (C=S). ^{1}H NMR (DMSO-d_6; δ, ppm): 12.60 (s, 1H, CSN$\underline{H}$); 10.80 (s, 1H, PhN$\underline{H}$); 8.63 (s, 1H, $\underline{H}$C=N); 8.48 (d, 2H, Ar$\underline{H}$, J = 8.27 Hz, *meta* protons to -OCF$_3$ group); 8.37 (d, 2H, Ar$\underline{H}$, J = 8.65 Hz, *orto* protons to -CN group); 8.27 (d, 2H, Ar$\underline{H}$, J = 8.66 Hz, *meta* protons to -CN group); 7.86 (d, 2H, Ar$\underline{H}$, J = 8.22 Hz, *orto* protons to -OCF$_3$ group). ^{13}C NMR (DMSO-d_6; δ, ppm): 176.24 ($\underline{C}$=S), 146.45 (Ar$\underline{C}$, *ipso* carbon to OCF$_3$), 142.76 ($\underline{C}$=N), 140.37, 139.63, 131.85, 128.79 (Ar$\underline{C}$), 126.41 (O$\underline{C}$F$_3$), 124.19, 123.07, 115.54 (Ar$\underline{C}$), 107.05 (C≡N).

2-(4-Fluorobenzylidene)-*N*-(4-cyanophenyl)hydrazinecarbothioamide (Ie). White solid (acetone). Yield: 0.23 g (73%); m.p.: 206 – 207°C. IR (ν_{max}, cm^{-1}): 3284, 3146 (N-H); 2226 (C≡N); 1581 (C=N); 1201 (C-N); 1076 (N-N); 827 (C=S). ^{1}H NMR (DMSO-d_6; δ, ppm): 12.51 (s, 1H, CSN$\underline{H}$); 10.73 (s, 1H, PhN$\underline{H}$); 8.61 (s, 1H, $\underline{H}$C=N); 8.42 (dd, 2H, Ar$\underline{H}$, J = 8.79 Hz, *meta* protons to -F atom); 8.37 (d, 2H, Ar$\underline{H}$, J = 8.74 Hz, *orto* protons to -CN group); 8.26 (d, 2H, Ar$\underline{H}$, J = 8.73 Hz, *meta* protons to -CN group); 7.72 (t, 2H, Ar$\underline{H}$, J = 8.86 Hz, *orto* protons to -F atom). ^{13}C NMR (DMSO-d_6; δ, ppm): 176.71 ($\underline{C}$=S), 163.99 (Ar$\underline{C}$, *ipso* carbon to -F atom), 142.77 ($\underline{C}$=N), 139.78, 134.14, 132.42, 130.23, 126.47, 118.53, 116.77 (Ar$\underline{C}$), 106.96 (C≡N).

2-(4-Nitrobenzylidene)-*N*-(4-cyanophenyl)hydrazinecarbothioamide (If). Dark yellow solid (ethanol). Yield: 0.27 g (81%); m.p.: 256 – 257°C. IR (ν_{max}, cm^{-1}): 3280, 3140 (N-H); 2224 (C≡N); 1579 (C=N); 1499 (NO$_2$, asymmetric); 1337 (NO$_2$, symmetric); 1200 (C-N); 1088 (N-N); 839 (C=S). ^{1}H NMR (DMSO-d_6; δ, ppm): 12.35 (s, 1H, CSN$\underline{H}$); 10.51 (s, 1H, PhN$\underline{H}$); 8.31 (d, 2H, Ar$\underline{H}$, J = 8.86 Hz, *orto* protons to -NO$_2$ group); 8.28 (s, 1H, $\underline{H}$C=N); 8.21 (d, 2H, Ar$\underline{H}$, J = 8.87 Hz, *meta* protons to -NO$_2$ group); 7.95 (d, 2H, Ar$\underline{H}$, J = 8.62 Hz, *orto* protons to -CN group); 7.82 (d, 2H, Ar$\underline{H}$, J = 8.65 Hz, *meta* protons to -CN group). ^{13}C

NMR (DMSO-d_6; δ, ppm): 176.39 ($\underline{C}$=S); 148.23 (Ar$\underline{C}$, *ipso* carbon to -NO$_2$ group); 143.64 ($\underline{C}$=N); 141.62, 140.55, 132.71, 128.97, 125.88, 124.17, 119.27 (Ar$\underline{C}$), 107.53 (C≡N).

2-{4-[Bis(2-chloroethyl)amino]benzylidene}-*N*-(4-cyanophenyl)hydrazinecarbo thioamide (Ig). Light brown solid (acetone). Yield: 0.33 g (76%); m.p.: 174 – 175°C. IR (ν_{max}, cm^{-1}): 3290, 3148 (N-H); 2228 (C≡N); 1582 (C=N); 1199 (C-N); 1076 (N-N); 829 (C=S); 719 (C-Cl). ^{1}H NMR (DMSO-d_6; δ, ppm): 11.90 (s, 1H, CSN$\underline{H}$); 10.18 (s, 1H, PhN$\underline{H}$); 8.08 (s, 1H, $\underline{H}$C=N); 7.99 (d, 2H, Ar$\underline{H}$, J = 8.50 Hz, *orto* protons to -CN group); 7.81 (d, 2H, Ar$\underline{H}$, J = 8.53 Hz, *meta* protons to -CN group); 7.73 (d, 2H, Ar$\underline{H}$, J = 8.70 Hz, *meta* protons to -N(CH$_2$CH$_2$Cl)$_2$ group); 6.81 (d, 2H, Ar$\underline{H}$, J = 8.75 Hz, *orto* protons to -N(CH$_2$CH$_2$Cl)$_2$ group); 3.76 – 3.81 (m, 8H, -N(C$\underline{H}_2$C$\underline{H}_2$Cl)$_2$). ^{13}C NMR (DMSO-d_6; δ, ppm): 176.49 ($\underline{C}$=S), 149.25 (Ar$\underline{C}$, *ipso* carbon to -N(CH$_2$CH$_2$Cl)$_2$ group), 143.33 ($\underline{C}$=N), 136.64, 134.12, 130.45, 127.68, 125.96, 123.87, 112.65 (Ar$\underline{C}$), 107.78 (C≡N), 53.18 (N(CH$_2$$\underline{C}H_2$Cl)$_2$), 42.54 (N($\underline{C}H_2CH_2$Cl)$_2$).

2-Benzylidene-*N*-[(4-methylthio)phenyl]hydrazinecarbothioamide (IIa). White solid (acetone). Yield: 0.27 g (85%); m.p.: 211 – 212°C. IR (ν_{max}, cm^{-1}): 3299, 3149 (N-H); 1573 (C=N); 1082 (C-N); 1062 (N-N); 823 (C=S). ^{1}H NMR (DMSO-d_6; δ, ppm): 11.84 (s, 1H, CSN$\underline{H}$); 10.09 (s, 1H, PhN$\underline{H}$); 8.17 (s, 1H, $\underline{H}$C=N); 7.91 (dd, 2H, Ar$\underline{H}$, J_1 = 3.80 Hz, J_2=2.05 Hz, *orto* protons at phenyl ring); 7.53 (d, 2H, Ar$\underline{H}$, J = 8.58 Hz, *meta* protons to -SCH$_3$ group); 7.44 (t, 3H, Ar$\underline{H}$, J_1 = 3.47 Hz, J_2=2.27 Hz, *para* and *meta* protons at phenyl ring); 7.28 (d, 2H, Ar$\underline{H}$, J = 8.59 Hz, *orto* protons to -SCH$_3$ group), 2.49 (s, 3H, SC$\underline{H}_3$). ^{13}C NMR (DMSO-d_6; δ, ppm): 174.23 ($\underline{C}$=S), 143.85 ($\underline{C}$=N), 135.47, 134.92, 133.76, 131.67, 131.01, 129.28, 128.85, 125.71 (Ar$\underline{C}$), 15.43 (S$\underline{C}$H$_3$).

2-(4-Hydroxybenzylidene)-*N*-[(4-methylthio)phenyl]hydrazinecarbothioamide (IIb). White solid (methanol). Yield: 0.26 g (81%); m.p.: 202 – 203°C. IR (ν_{max}, cm^{-1}): 3580 (O-H); 3266, 3153 (N-H); 1583 (C=N); 1164 (C-N); 1069 (N-N); 818 (C=S). ^{1}H NMR (DMSO-d_6; δ, ppm): 11.65 (s, 1H, CSN$\underline{H}$); 9.94 (s, 1H, PhN$\underline{H}$); 9.92 (s, 1H, O$\underline{H}$); 8.07 (s, 1H, $\underline{H}$C=N); 7.73 (d, 2H, Ar$\underline{H}$, J = 8.59 Hz, *meta* protons to -OH group); 7.54 (d, 2H, Ar$\underline{H}$, J = 8.57 Hz, *meta* protons to -SCH$_3$ group); 7.26 (d, 2H, ArH, J = 8.59 Hz, *orto* protons to -OH group); 6.81 (d, 2H, Ar$\underline{H}$, J = 8.57 Hz *orto* protons to -SCH$_3$ group), 2.49 (s, 3H, SC$\underline{H}_3$). ^{13}C NMR (DMSO-d_6; δ, ppm): 176.92 ($\underline{C}$=S), 153.29 (Ar$\underline{C}$, *ipso* carbon to -OH group), 142.57 ($\underline{C}$=N), 131.27, 129.62, 128.51, 126.13, 125.48, 120.03, 115.68 (Ar$\underline{C}$), 16.67 (S$\underline{C}$H$_3$).

2-(4-Methoxyybenzylidene)-*N*-[(4-methylthio)phenyl]hydrazinecarbothioamide (IIc). White solid (acetone). Yield: 0.25 g (73%); m.p.: 194 – 195°C. IR (ν_{max}, cm^{-1}): 3309, 3126 (N-H); 1570 (C=N); 1164 (C-N); 1068 (N-N); 823 (C=S). ^{1}H NMR (DMSO-d_6; δ, ppm): 11.72 (s, 1H, CSN$\underline{H}$); 10.01 (s, 1H, PhN$\underline{H}$); 8.11 (s, 1H, $\underline{H}$C=N); 7.85 (d,

2H, Ar$\underline{H}$, $J = 8.74$ Hz, *meta* protons to -SCH$_3$ group); 7.53 (d, 2H, Ar$\underline{H}$, $J = 8.57$ Hz, *meta* protons to -OCH$_3$ group); 7.27 (d, 2H, Ar$\underline{H}$, $J = 8.57$ Hz, *orto* protons to -OCH$_3$ group); 6.99 (d, 2H, Ar$\underline{H}$, $J = 8.74$ Hz, *orto* protons to -SCH$_3$ group); 3.81 (s, 3H, OC$\underline{H}_3$), 2.49 (s, 3H, SC$\underline{H}_3$). ^{13}C NMR (DMSO-d_6; δ, ppm): 175.93 (C=S), 161.25 (Ar$\underline{C}$, *ipso* carbon to -OCH$_3$ group), 143.36 (C=N), 136.67, 134.83, 129.66, 126.83, 126.73, 126.10, 114.51 (Ar$\underline{C}$), 55.70 (O$\underline{C}$H$_3$), 15.44 (S$\underline{C}$H$_3$).

2-[(4-Trifluoromethoxy)benzylidene]-*N*-[(4-methyl-thio)phenyl]hydrazinecarbo thioamide (IId). White solid (chloroform). Yield: 0.25 g (74%); m.p.: 198 – 199°C. IR (ν$_{max}$, cm^{-1}): 3324, 3121 (N-H); 1577 (C=N); 1160 (C-N); 1077 (N-N); 822 (C=S). ^{1}H NMR (DMSO-d_6; δ, ppm): 11.91 (s, 1H, CSN$\underline{H}$); 10.15 (s, 1H, PhN$\underline{H}$); 8.17 (s, 1H, $\underline{H}$C=N); 8.06 (d, 2H, Ar$\underline{H}$, $J = 8.57$ Hz, *meta* protons to -SCH$_3$ group); 7.51 (d, 2H, Ar$\underline{H}$, $J = 8.55$ Hz, *meta* protons to -OCF$_3$ group); 7.42 (d, 2H, Ar$\underline{H}$, $J = 8.52$ Hz, *orto* protons to -OCF$_3$ group); 7.28 (d, 2H, Ar$\underline{H}$, $J = 8.56$ Hz, *orto* protons to -SCH$_3$ group); 2.49 (s, 3H, -SC$\underline{H}_3$). ^{13}C NMR (DMSO-d_6; δ, ppm): 176.40 ($\underline{C}$=S), 147.36 (Ar$\underline{C}$, *ipso* carbon to -OCF$_3$ group), 143.71 ($\underline{C}$=N), 141.11, 139.78, 136.33, 129.81 (Ar$\underline{C}$), 127.04 (O$\underline{C}$F$_3$), 125.92, 122.49, 116.12 (Ar$\underline{C}$), 15.84 (S$\underline{C}$H$_3$).

2-(4-Fluorobenzylidene)-*N*-[(4-methylthio)phenyl]hyd-razinecarbothioamide (IIe). White solid (chloroform). Yield: 0.24 g (72%); m.p.: 175 – 176°C. IR (ν$_{max}$, cm^{-1}): 3323, 3133 (N-H); 1581 (C=N); 1228 (C-F); 1150 (C-N); 1069 (N-N); 826 (C=S). ^{1}H NMR (DMSO-d_6; δ, ppm): 11.83 (s, 1H, CSN$\underline{H}$); 10.11 (s, 1H, PhN$\underline{H}$); 8.15 (s, 1H, $\underline{H}$C=N); 7.99 (dd, 2H, Ar$\underline{H}$, $J = 8.70$ Hz, *meta* protons to -F atom); 7.51 (d, 2H, Ar$\underline{H}$, $J = 8.57$ Hz, *meta* protons to -SCH$_3$ group); 7.28 (t, 2H, Ar$\underline{H}$, $J = 8.77$ Hz, *orto* protons to -F atom); 7.27 (d, 2H, Ar$\underline{H}$, $J = 8.55$ Hz, *orto* protons to -SCH$_3$ group); 2.49 (s, 3H, -SC$\underline{H}_3$). ^{13}C NMR (DMSO-d_6; δ, ppm): 176.89 ($\underline{C}$=S), 164.01 (Ar$\underline{C}$, *ipso* carbon to -F atom), 143.18 ($\underline{C}$=N), 140.04, 133.95, 131.56, 130.19, 127.76, 119.31, 115.83 (Ar$\underline{C}$), 16.24 (S$\underline{C}$H$_3$).

2-(4-Nitrobenzylidene)-*N*-[(4-methylthio)phenyl]hyd-razinecarbothioamide (IIf).

Orange solid (acetone). Yield: 0.30 g (82%); m.p.: 225 – 226°C. IR (ν$_{max}$, cm^{-1}): 3296, 3120 (N-H); 1587 (C=N); 1435 (NO$_2$, asymmetric); 1336 (NO$_2$, symmetric); 1185 (C-N); 1083 (N-N); 836 (C=S). ^{1}H NMR (DMSO-d_6; δ, ppm): 12.10 (s, 1H, CSN$\underline{H}$); 10.30 (s, 1H, PhN$\underline{H}$); 8.27 (d, 2H, Ar$\underline{H}$, $J = 8.96$ Hz, *orto* protons to -NO$_2$ group); 8.24 (s, 1H, $\underline{H}$C=N); 8.21 (d, 2H, Ar$\underline{H}$, $J = 8.95$ Hz, *meta* protons to -NO$_2$ group); 7.50 (d, 2H, Ar$\underline{H}$, $J = 8.58$ Hz, *meta* protons to -SCH$_3$ group); 7.29 (d, 2H, Ar$\underline{H}$, $J = 8.59$ Hz, *orto* protons to -SCH$_3$ group); 2.50 (s, 3H, -SC$\underline{H}_3$). ^{13}C NMR (DMSO-d_6; δ, ppm): 176.57 ($\underline{C}$=S), 149.15 (Ar$\underline{C}$, *ipso* carbon to -NO$_2$ group), 142.86 ($\underline{C}$=N), 140.54, 139.27, 133.66, 130.83, 129.11, 128.77, 126.35 (Ar$\underline{C}$), 15.88 (S$\underline{C}$H$_3$).

2-{4-[Bis(2-chloroethyl)amino]benzylidene}-*N*-[(4-me-thylthio)phenyl]hydrazine carbothioamide (IIg). Light

yellow solid (chloroform). Yield: 0.40 g (88%); m.p.: 192 – 193°C. IR (ν$_{max}$, cm^{-1}): 3299, 3162 (N-H); 2228 1545 (C=N); 1177 (C-N); 1061 (N-N); 818 (C=S); 712 (C-Cl). ^{1}H NMR (DMSO-d_6; δ, ppm): 11.62 (s, 1H, CSN$\underline{H}$); 9.92 (s, 1H, PhN$\underline{H}$); 8.04 (s, 1H, $\underline{H}$C=N); 7.72 (d, 2H, Ar$\underline{H}$, $J = 8.82$ Hz, *meta* protons to -SCH$_3$ group); 7.55 (d, 2H, Ar$\underline{H}$, $J = 8.58$ Hz, *meta* protons to -N(CH$_2$CH$_2$Cl)$_2$ group); 7.26 (d, 2H, Ar$\underline{H}$, $J = 8.60$ Hz, *orto* protons to -N(CH$_2$CH$_2$Cl)$_2$ group); 6.80 (d, 2H, Ar$\underline{H}$, $J = 8.90$ Hz, *orto* protons to -SCH$_3$ group); 3.75 – 3.82 (m, 8H, -N(C$\underline{H}_2$C$\underline{H}_2$Cl)$_2$ protons); 2.50 (s, 3H, -SC$\underline{H}_3$). ^{13}C NMR (DMSO-d_6; δ, ppm): 175.96 ($\underline{C}$=S), 148.41 (Ar$\underline{C}$, *ipso* carbon to -N(CH$_2$CH$_2$Cl)$_2$ group), 143.89 ($\underline{C}$=N), 136.70, 134.56, 129.72, 126.44, 126.12, 122.63, 112.06 (Ar$\underline{C}$), 52.32 (N(CH$_2$$\underline{C}H_2$Cl)$_2$), 41.87 (N($\underline{C}H_2CH_2$Cl)$_2$), 15.57 (S$\underline{C}H_3$).

3. EXPERIMENTAL BIOLOGICAL PART

3.1. Antiviral Activity Assay

The antiviral assays were based on the inhibition of virus-induced cytopathicity in confluent cell cultures, and the cytostatic assays on inhibition of tumor cell proliferation in exponentially growing tumor cell cultures according to previously described methods [17]. The synthesized compounds were evaluated against the following viruses: herpes simplex virus type 1 (HSV-1) strain KOS, thymidine kinase-deficient (TK–) HSV-1 KOS strain resistant to ACV (ACV^r), herpes simplex virus type 2 (HSV-2) strain G, cytomegalovirus strains AD-169 and David, varicella zoster virus (VZV) strains OKA and YS, vaccinia virus Lederle strain, respiratory syncytial virus (RSV) strain Long, vesicular stomatitis virus (VSV), Coxsackie B4 virus, parainfluenza 3 virus, influenza virus A (subtypes H1N1, H3N2), influenza virus B, reovirus-1, Sindbis and Punta Toro virus. The antiviral assays were based on inhibition of virus-induced cytopathicity or plaque formation (for VZV) in human embryonic lung (HEL) fibroblasts, African green monkey cells (Vero), human epithelial cervix carcinoma cells (HeLa) or Madin-Darby canine kidney cells (MDCK). Confluent cell cultures in microtiter 96-well plates were inoculated with 100 CCID$_{50}$ of virus (1 CCID$_{50}$ being the virus dose to infect 50% of the cell cultures) or 20 or 100 plaque forming units (PFU) (for VZV and CMV, respectively) in the presence of varying concentrations of the test compounds. Viral cytopathicity or plaque formation was recorded as soon as it reached completion in the control virus-infected cell cultures that were not treated with the test compounds. Antiviral activity was expressed as EC$_{50}$ (50% effective concentration) defined as the compound concentration required to reduce virus-induced cytopathogenicity or viral plaque formation by 50%). Inhibition of HIV-1(III$_B$)- and HIV-2(ROD)-induced cytopathicity in CEM cell cultures was measured in microtiter 96-well plates containing ~3 × 10^5 CEM cells/mL

infected with 100 CCID$_{50}$ of HIV per milliliter and containing appropriate dilutions of the test compounds. After 4 – 5 days of incubation at 37°C in a CO$_2$-controlled humidified atmosphere, CEM giant (syncytium) cell formation was examined microscopically and characterized by the EC$_{50}$ value (50% effective concentration inhibiting HIV-induced giant cell formation by 50%).

3.2. Cytostatic/Toxic Activity Assay

All cytostatic/toxic activity assays were performed in 96-well microliter plates. To each well were added (5 – 7.5) × 10^4 tumor cells and a given amount of the test compound. The cells were allowed to proliferate for 48 h (murine leukemia L1210 cells) or 72 h (human CD$_4^+$ T-lymphocytic CEM and human cervix carcinoma HeLa cells) at 37°C in a humidified CO$_2$-controlled atmosphere. At the end of the incubation period, the cells were counted in a Coulter counter. The IC$_{50}$ (50% inhibitory concentration) was defined as the concentration of the compound that inhibited cell proliferation by 50%. Cisplatin was purchased from SIGMA and used as a reference drug. Compound concentrations of 100, 20, 4, 0.8, 0.16 and 0.032 µg/mL have been tested (5-fold dilutions) and the data represent the mean ± SD (standard deviation) of at least two to three independent experiments. All values are significantly different from cisplatin (less active), except for **Ig** (no statistical difference, $p > 0.05$).

4. EXPERIMENTAL MOLECULAR MODELING PART

The biological activity depended on only on the chemical structure of substituents, but also on the three dimensional (3D) configuration of compound **Ig**. For this reason, we again applied computational methods and ligand-based pharmacophore modeling to evaluate this state. The new derivatives of thiosemicarbazones (**Ia – Ig** and **IIa – IIg**) were drawn and converted from 2D to 3D, and the PM3MM basis set was assigned and then minimized using a semi-empirical method with the aid of Gaussian09 program package. A conformational search of the ligands was carried out using BEST algorithm for 3D pharmacophore generation. The Auto Pharmacophore Generation protocol in Discovery Studio 3.5 was used based on a bioactive conformation. In this study, we used compound **Ig** as the bioactive conformation with IC$_{50}$ values between 0.30 and 2.50 µg/mL. The pharmacophore models were generated based on the main features of compound **Ig**. These features were Hb-Acceptor, Hb-Donor, Hydrophobic and Ring Aromatic in the pharmacophore models. Besides, the Genetic Function Approximation (GFA) model for the selectivity of pharmacophores was used. The best model was determined with the help of Clusters pharmacophores subprotocol. The model contains six features, representing two hydrophobic

(cyan), two ring aromatic (orange), one hydrogen bond donor (pink) and one hydrogen acceptor (green).

5. RESULTS AND DISCUSSION

All newly synthesized compounds were evaluated for their antiviral, cytostatic, and cytotoxic properties. None of the compounds effectively inhibited DNA virus replication (i.e. HSV-1, HSV-2, VV), except **I** and **II** that showed slight activity against vaccinia virus replication in HEL cell cultures (EC$_{50}$ = 45 – 50 µg/mL) and compounds **Ib**, **Ic** and **IIc** bearing an electron-donating group (–OH and –OCH$_3$) against feline herpes virus (EC$_{50}$ = 17.8 – 54.3 µg/mL). All compounds were also not significantly inhibitory against a wide variety of RNA viruses, including vesicular stomatitis virus (VSV), respiratory syncytial virus and Coxsackie virus in HeLa cell cultures at subtoxic concentrations (Table 2). However, in Vero cell cultures compound **Ig** consistently showed an antiviral activity of 3 µg/mL (EC$_{50}$) against Coxsackie virus B4 but there was no inhibitory activity observed for parainfluenza virus-3, reovirus-1, Sindbis virus and Punta Toro virus (Table 2). The fact that the activity of **Ig** against Coxsackie virus B4 was only observed in one cell line (monkey kidney Vero), but not in another cell line (human cervix carcinoma HeLa) led us to conclude that this compound should not be considered as a consistent new antiviral lead agent.

A marginal activity was observed for **Ib**, **Ic** and **IIc** against feline herpes virus (EC$_{50}$ = 17.8 – 54.3 µg/mL) and for **Ib**, **Ic** and **IIa** against feline corona (FIPV) virus (EC$_{50}$ = 7.0 – 31.5 µg/mL) in CRFK cell cultures (Table 3). Whereas no activity was found in MDCK cell cultures against influenza B virus, compounds **Id**, **Ie**, **If** and **IIf** which have an electron-withdrawing group (–CF$_3$, –F and –NO$_2$) proved inhibitory against influenza A virus (EC$_{50}$: 12.7 – 26.7 µg/mL for strain H1N1 and 9.3 – 18.5 µg/mL for strain H3N2). These compounds were only 5- to 20-fold less effective than the clinically used drug oseltamivir and were neither cytotoxic (MCC) nor cytostatic (CC$_{50}$) at 100 µg/mL against MDCK cells (Table 3). Thus, a certain degree of selectivity was present for these compounds against influenza A virus in cell culture and should be further considered for optimization as potential anti-influenza virus lead compounds.

The synthesized compounds were also evaluated for their cytostatic activity against murine leukemia L1210, human CD$_4^+$ T-lymphocyte CEM and cervix carcinoma HeLa cells (Table 4). Most compounds in the **IIa – IIg** series did not show pronounced cytostatic activity (IC$_{50}$ ≥ 100 µg/mL). However, **IIb** was moderately cytostatic (IC$_{50}$ = 13 – 15 µg/mL), whereas **IIg** seemed to be poorly inhibitory to L1210 and CEM cell proliferation, but had a pronounced antiproliferative activity against HeLa cells (IC$_{50}$ = 1.9 µg/mL). This unusual selectivity between tumor cell lines should be further investigated. In fact, the **I** series of

compounds were often somewhat more cytostatic than their corresponding **II** series of compounds. It may not be a coincidence that **Ig** (IC$_{50}$ = 0.3 μg/mL against HeLa cells) was also most cytostatic among series **I** and also showed the most pronounced antiproliferative potency against HeLa cells.

The structure – activity relationship (SAR) studies were performed to determine how the substituent on the benzene ring affected the cytostatic activity. Compounds **Ia** and **IIa** without any substituent group on the benzene ring did not show cytostatic activity. Then, we examined the effect of introducing various substituent groups in the benzene ring of compounds **Ia** and **IIa**. The -OH, -OCH$_3$, -CF$_3$, -F, -NO$_2$ and -N(CH$_2$CH$_2$Cl)$_2$ groups at the *para* position of the benzene ring of compounds **Ia** and **IIa** were used to form compounds

TABLE 2. Cytotoxicity and Antiviral Activity of Thiosemicarbazides (**I** and **II**) and thiosemicarbazones (**Ia – Ig** and **IIa – IIg**) in HEL, HeLa and Vero Cell Cultures

| Compound | HEL cell culture | | | | | | HeLa cell culture | | | | Vero cell culture | | | | | |
| | MCC[a] (μg/mL) | EC$_{50}$[b] (μg/mL) | | | | | MCC[a] (μg/mL) | EC$_{50}$[b] (μg/mL) | | | MCC[a] (μg/mL) | EC$_{50}$[b] (μg/mL) | | | | |
		Herpes simpex virus-1 (KOS)	Herpes simplex virus-2 (G)	Vaccinia virus	Vesicular stomatitis virus	Herpes simplex virus-1 TK KOS ACV^r		Vesicular stomatitis virus	Coxsackie virus B4	Respiratory syncytial virus		Para influenza-3 virus	Reo virus-1	Sindbis virus	Coxsackie virus B4	Punta Toro virus
I	>100	>100	>100	**50**	>100	>100	≥100	>100	>100	>100	100	>20	>20	>20	>20	>20
Ia	>100	>100	>100	>100	>100	>100	≥100	>100	>100	>100	>100	>100	>100	>100	>100	>100
Ib	100	>20	>20	>20	>20	>20	100	>20	>20	>20	100	>20	>20	>20	>20	>20
Ic	>100	>100	>100	>100	>100	>100	100	>20	>20	>20	100	>20	>20	>20	>20	>20
Id	>100	>100	>100	>100	>100	>100	100	>20	>20	>20	100	>20	>20	>20	>20	>20
Ie	>100	>100	>100	>100	>100	>100	≥100	>100	>100	>100	100	>20	>20	>20	>20	>20
If	>100	>100	>100	>100	>100	>100	≥100	>100	>100	>100	>100	>100	>100	>100	>100	>100
Ig	>100	>100	>100	>100	>100	>100	≥20	>20	>20	>20	>20	>4	>4	>4	**3**	>4
II	>100	>100	>100	**45**	>100	100	100	>20	>20	>20	100	>20	>20	>20	>20	>20
IIa	100	>20	>20	>20	>20	>20	100	>20	>20	>20	100	>20	>20	>20	>20	>20
IIb	>100	>100	>100	>100	>100	>100	>100	>100	>100	>100	>100	>100	>100	>100	>100	>100
IIc	>100	>100	>100	>100	>100	>100	100	>20	>20	>20	100	>20	>20	>20	>20	>20
IId	100	>20	>20	>20	>20	>20	>100	>100	>100	>100	100	>20	>20	>20	>20	>20
IIe	100	>20	>20	>20	>20	>20	>100	>100	>100	>100	100	>20	>20	>20	>20	>20
IIf	>100	>100	>100	>100	>100	>100	100	>20	>20	>20	100	>20	>20	>20	>20	>20
IIg	100	>20	>20	>20	>20	>20	≥100	>100	>100	>100	100	>20	>20	>20	>20	>20
Brivudin (μM)	>250	0.04	100	10	>250	100										
Cidofovir (μM)	>250	2	2	29	>250	2										
Acyclovir (μM)	>250	0.4	0.2	>250	>250	112										
Ganciclovir (μM)	>100	0.03	0.06	>100	>100	10										
DS-5000[c]							>100	2	34	0.6	>100	>100	>100	100	9	100
(S)-DHPA[d] (μM)							>250	>250	>250	>250	>250	>250	>250	>250	>250	>250
Ribavirin (μM)							>250	5	112	10	>250	112	>250	>250	>250	146

[a] Required to cause a microscopically detectable alteration of normal cell morphology.
[b] Required to reduce virus-induced cytopathogenicity by 50%.
[c] DS-5000: dextran sulfate (molecular weight, 5.000).
[d] (S)-DHPA: (S)-9-(2,3-dihydroxypropyl)adenine.

(**Ib – Ig** and **IIb – IIg**). Especially **Ig** with a bis(2-chloro-ethyl)amino moiety, the IC_{50} values (0.30 – 2.50 µg/mL) were the lowest (most effective) among all compounds and compared to cisplatin as a reference compound. A two-tailed, unpaired t-test (GraphPad Prism) revealed no significant difference between the cytostatic inhibition values of **Ig** and cisplatin obtained against the three tumor cell lines ($p = 0.647$). The results showed that compounds **Ia – Ig** containing electron-withdrawing group, such as -CN located at the *para* position of the benzene ring, increased the cytostatic activity, according to the electron-donating group (-SCH$_3$) at the same position of the structure (like compounds

TABLE 3. Cytotoxicity and Antiviral Activity of Thiosemicarbazides (**I** and **II**) and Thiosemicarbazones (**Ia – Ig** and **IIa – IIg**) in CRFK and MDCK Cell Cultures.

Compound	CRFK cell culture			MDCK cell culture							
	CC_{50}[a] (µg/mL)	EC_{50}[b] (µg/mL)		CC_{50}[a] (µg/mL)	MCC[c] (µg/mL)	EC_{50}[b] (µg/mL)					
		Feline Corona Virus (FIPV)	Feline Herpes Virus			Influenza RH1N1 SUBTYPE		Influenza A H3N2 subtype		Influenza B	
						visual CPE score	MTS	visual CPE score	MTS	visual CPE score	MTS
I	84.6	>20	>20	78.6	100	>20	>20	>20	>20	>20	>20
Ia	>100	>100	>100	44.3	≥20	>20	>20	>20	>20	>20	>20
Ib	>100	**31.5**	54.3	>100	100	>20	>20	>20	>20	>20	>20
Ic	>100	**23.1**	25.0	>100	100	>20	>20	>20	>20	>20	>20
Id	>100	>100	>100	>100	>100	**27.0**	26.3	9.5	13.9	>100	>100
Ie	>100	>100	>100	>100	>100	**14.5**	10.9	23.0	14.0	>100	>100
If	>100	>100	>100	>100	>100	**10.5**	17.1	15.0	17.5	>100	>100
Ig	>100	>100	>100	0.4	0.8	>0.16	>0.16	>0.16	>0.16	>0.16	>0.16
II	>100	>100	>100	90.2	100	>20	>20	>20	>20	>20	>20
IIa	>100	**7.0**	>100	>100	100	>20	>20	>20	>20	>20	>20
IIb	>100	>100	>100	0.8	0.8	>0.16	>0.16	>0.16	>0.16	>0.16	>0.16
IIc	>100	>100	**17.8**	>100	100	>20	>20	>20	>20	>20	>20
IId	>100	>100	>100	>100, ≥20100	>100	>100	>100	>100	>100	>100	
IIe	>100	>100	>100	>100, ≥20100	>100	>100	>100	>100	>100	>100	
IIf	>100	>100	>100	>100	>100	**11.0**	16.5	9.0	9.5	>100	>100
IIg	>100	>100	>100	>100	>100	>100	>100	>100	>100	>100	>100
HHA[d]	>100	36.2	16.5								
UDA[e]	33.2	1.6	1.8								
Ganciclovir (µM)	>100	>100	7.3								
Oseltamivir carboxylate				>100	>100	2.0	2.7	1.0	0.8	34.0	29.1
Ribavirin				>100	>100	9.0	8.3	9.0	5.7	9.0	3.4
Amandatine				>200	>200	8.0	5.4	0.9	0.3	>200	>200
Rimandatine				>200	>200	18.0	25.7	0.9	0.4	>200	>200

[a] 50% Cytotoxic concentration, as determined by measuring the cell viability with the colorimetric formazan- based MTS assay.
[b] 50% Effective concentration, or concentration producing 50% inhibition of virus-induced cytopathic effect, as determined by measuring the cell viability with the colorimetric formazan-based MTS assay.
[c] Required to cause a microscopically detectable alteration of normal cell morphology.
[d] HHA: Hippeastrum hybrid Lectin (Amoryllis bulbs).
[e] UDA: Urtica dioica agglutinin.

IIa – IIg). Furthermore, the introduction of electron-donating groups (-OH, -OCH$_3$) at the *para* position of the benzene ring weakened the cytostatic effects. While the same situation for electron-withdrawing groups (-F, -NO$_2$, -CF$_3$) was also observed, compound **IIb** exhibited moderate activity against all tumor cell types. Besides, compound **1g** displayed the better cytostatic activity than its analog compound **IIg**, which has an electron-donating group (-SCH$_3$) at the *para* position. These results indicated that the introduction of the bulky alkylating group (bis(2-chloroethyl)amino) and a cyano group reinforced the cytostatic activity.

The pharmacophore model (Fig. 2A) was hypothetically superimposed with compounds **Ig** (fit value 4.6216) and **IIg** (fit value 3.0032). Figures 2B and 2C summarize the results of model fitting obtained for compounds **Ig** and **IIg.** The other compounds were not superimposed to fit with the best model. In addition to comparing the results of modeling with experimental data, they show compatible and significant trends. It is established that Hb-acceptor (-CN; -SCH$_3$), hydrophobic groups (-N(CH$_2$CH$_2$Cl)$_2$), and 3D-conformations are responsible for the cytostatic activity of compounds such as **Ig** and **IIg**, according to ligand-based pharmacophore modeling. Especially, 3D-conformation of the investigated compounds showed the major effect in this study. Unfortunately, compounds **Ia – If** and **IIa – IIf** did not show any activity in comparison to compounds **Ig** and **IIg**. The proposed methods were able to provide valuable information about key features and interactions that are important for the biological activity of compound **Ig.** Thus, ligand-based pharmacophore modeling was increasingly successful in delineating why compound **Ig** displayed better cytostatic activity than compound **IIg.**

ACKNOWLEDGEMENTS

TABLE 4. Inhibitory Effect of Compounds **I**, **Ia – Ig** and **II, IIa – IIg** on the Proliferation of Murine Leukemia (L1210), Human CD$_4^+$ T-Lymphocyte (CEM) and Human Cervix Carcinoma (HeLa) Cells

Compound	IC$_{50}$[a] (µg/mL)		
	L1210	CEM	HeLa
I	20 ± 3	21 ± 1	11 ± 0
Ia	79 ± 48	83 ± 59	67 ± 10
Ib	50 ± 2	107 ± 13	91 ± 18
Ic	>200	>200	31 ± 23
Id	>200	>200	>200
Ie	29 ± 12	38 ± 27	68 ± 9
If	>200	>200	142 ± 20
Ig	**2.5 ± 0.2**	**0.70 ± 0.16**	**0.30 ± 0.17**
II	83 ± 24	20 ± 0	18 ± 8
IIa	>200	>200	185 ± 21
IIb	14 ± 4	15 ± 14	13 ± 2
IIc	>200	121 ± 24	112 ± 8
IId	≥ 200	145 ± 68	61 ± 5
IIe	>200	≥ 200	>200
IIf	>200	>200	>200
IIg	≥ 200	50 ± 23	**1.9 ± 1.7**
Cisplatin[b]	2.53 ± 0.3	2.20 ± 0.1	0.22 ± 0.03

[a] 50%-Inhibitory concentration or compound concentration required to inhibit tumor cell proliferation by 50%. Compound concentration of 100, 20, 4, 0.8, 0.16 and 0.032 µg/mL have been tested (5-fold dilutions) and data represent the mean ± SD (standard deviation) of at least two to three independent experiments. All values were significantly different from cisplatin (less active), except for **Ig** (no statistical difference, p higher than 0.05).
[b] Cisplatin was purchased from SIGMA.
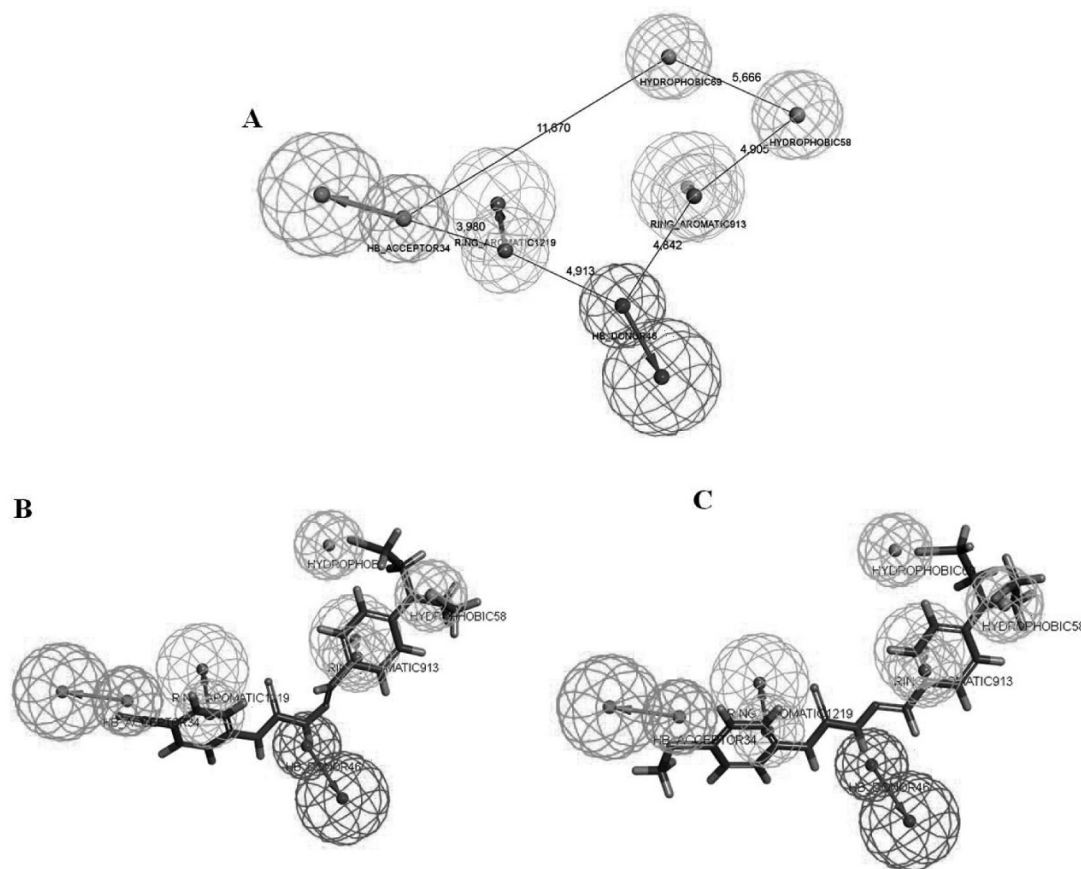
Fig. 2. (**A**) Pharmacophore model of the docking pose of compound **Ig**; (**B**) the mapping of compound **Ig** (fit value 4.6216) to hypo10; (C) the mapping of compound **IIg** (fit value 3.0032) to hypo10.

REFERENCES

1. G. Domagk, R. Behnisch, F. Mietzsch, et al., *Naturwissenschaften*, **33**, 315 (1946).
2. D. Hamre, J. Bernstein. and R. Donovick, *Proc. Soc. Exp. Biol. Med.*, **73**, 275 – 278 (1950).
3. D. J. Bauer, L. St. Vincent, C. H. Kempe, et al., *Lancet*, **2**, 494 – 496 (1963).
4. M. A. Soares, J. A., Lessa, I. C. Mendes, et al., *Bioorg. Med. Chem.,* **20**, 3396 – 3409. (2012).
5. R. A. Finch, M.-C. Liu, S. P. Grill, et al. *Biochem. Pharmacol.,* **59**, 983 – 991 (2000).
6. V. R. Solomon, C. Hu, and H. Lee, *Bioorg. Med. Chem.,* **18**, 1563 – 1572 (2010).
7. D. M. Noll, T. M. Mason, and P. S. Miller, *Chem. Rev.,* **106**, 277 – 301 (2006).
8. F. F. Fleming, L. Yao, P. C. Ravikumar, et al. *J. Med. Chem.,* **53**, 7902 – 7917 (2010).
9. A. Karaküçük-Iyidoğan, D. Taşdemir, E. E. Oruç-Emre, et al., *Eur. J. Med. Chem.,* **46**, 5616 – 5624 (2011).
10. M. J. Frisch, G. W. Trucks, H. B. Schlegel, et al. Gaussian 09, Revision A.1 Gaussian, Inc., Wallingford CT (2009).
11. Accelrys Software Inc., Discovery Studio 3.5, San Diego (2013).
12. A. Karaküçük-Iyidoğan, Z. Mercan, E. E. Oruç-Emre, et al. *Phosphorus Sulfur and Silicon,* **189**, 661 – 673 (2014).
13. H. Huang, Q. Chen, X. Ku, et al., *J. Med. Chem.,* **53**, 3048 – 3064 (2010).
14. M. Leigh, D. J. Raines, C.E. Castillo, et al. *Chem. Med. Chem.,* **6**, 1107 – 1118 (2011).
15. A.-C. Tnechiu (Deleanu), I. D. Kostas, D. Kovala-Demertzi, et al. *Carbohydr. Res.,* **344**, 1352 – 1364 (2009).
16. V. A. Chornous, A. N. Grozav, L. D. Todoriko, et al. *Pharm. Chem. J.,* **47**(10), 524 – 526 (2014).
17. E. Tsoukala, N. Tzioumaki, S. Manta, et al. *Bioorg. Chem.*, **38**, 285 – 293 (2010).